

---

## Irradiated Fuel Measurements

---

*J. R. Phillips*

### 18.1 INTRODUCTION

There are over 100 nuclear power plants operating in the US with a total installed generating capacity of more than 85 GW (gigawatts, 1 GW =  $10^9$  W) (Ref. 1). These reactors discharge 5 000 to 10 000 irradiated fuel assemblies each year. Some of the assemblies are cooled for a year or two and then reinserted into the reactor to optimize the burnup of the residual fissile material; others, having reached their maximum design burnup, are placed in the storage pond at the reactor site until they are sent to a long-term storage facility or to a waste disposal site. These thousands of fuel assemblies are safeguarded by counting the individual assemblies and accepting the operator-declared values for the depletion of the initial fissile material ( $^{235}\text{U}$  or  $^{239}\text{Pu}$ ) and for the buildup of the fissile plutonium isotopes ( $^{239}\text{Pu}$  and  $^{241}\text{Pu}$ ). To augment this modest method of accountability, a variety of nondestructive measurement techniques have been developed for verifying the operator-declared values.

Before irradiation, power reactor fuels can be characterized using the gamma-ray and neutron measurement techniques discussed in Chapters 7, 8, 15, and 17. However, after a significant exposure of the fuel in the reactor, the uranium and plutonium signatures are completely masked by radiation from fission products, activated structural components, and transuranic elements that build up as a result of the fission process. Thus neither gamma-ray nor neutron measurements of irradiated fuel yield signatures for  $^{235}\text{U}$ ,  $^{239}\text{Pu}$ , or  $^{241}\text{Pu}$ . Instead, indirect signatures must be used to estimate these quantities. These indirect signatures are based on radiation from fission products or transuranic elements and are used to determine the burnup and cooling time of the irradiated fuel. From the burnup, the buildup of  $^{239}\text{Pu}$  and  $^{241}\text{Pu}$  in the fuel can then be estimated by calculational techniques.

It is also possible to use active neutron interrogation techniques to determine the amount of fissile material present in irradiated fuel assemblies. These measurement techniques require the use of a highly active neutron source (for example,  $^{252}\text{Cf}$ ) or an accelerator and generally require fixed, in-plant equipment.

This chapter describes the physical characteristics of reactor fuel (Section 18.2), indirect signatures for burnup (Section 18.3), and gamma-ray and neutron measurements of irradiated fuel (Sections 18.4 and 18.5). Section 18.6 summarizes passive and active methods for estimating the plutonium content of irradiated fuel.

## 18.2 CHARACTERISTICS OF REACTOR FUEL

### 18.2.1 Physical Description

With the exception of one high-temperature gas-cooled reactor (Fort St. Vrain), all power reactors presently operating in the US are either pressurized water reactors (PWRs) or boiling water reactors (BWRs). Research is under way on fast breeder reactors (FBRs). The fuel and core parameters of PWRs, BWRs, and FBRs are compared in Table 18-1 (Refs. 2 and 3). Figure 18.1 illustrates the differences in fuel pin and assembly sizes.

Reactor fuel initially consists of fissionable material ( $^{235}\text{U}$  or  $^{239}\text{Pu}$ ) plus fertile material ( $^{238}\text{U}$ ). These materials are usually present in ceramic oxide or carbide forms because of their improved corrosion characteristics, relative ease of fabrication, and better radiation-damage characteristics. In PWRs or BWRs the fuel is in the form of  $\text{UO}_2$  ceramic pellets that are about 1 cm in diameter and 2 cm in length. The pellets are stacked in a stainless steel or Zircaloy tubing to an active length of 3.7 m. Zircaloy is a zirconium alloy used in most PWR and BWR fuels because of its low neutron absorption cross section. The fuel is contained in a cladding material to protect it from chemical reaction with air, water, or other material used as coolant.

Table 18-1. Fuel and core parameters for reactors

	PWR	BWR	FBR
<b>Fuel Parameters</b>			
Cladding material	Zircaloy-4	Zircaloy-2	SS 316
Cladding diameter	0.95 cm	1.23 cm	0.74 cm
Cladding thickness	0.06 cm	0.08 cm	0.03 cm
Fuel material	$\text{UO}_2$	$\text{UO}_2$	$(\text{U,Pu})\text{O}_2$
$^{235}\text{U}$ initial enrichment	2.1/2.6/3.1%	2.8% average	25% Pu
Pellet diameter	0.82 cm	1.04 cm	0.67 cm
Pellet height	1.5 cm	1.04 cm	0.7 cm
Assembly array	15 × 15 or 17 × 17	8 × 8	hexagonal (17/side)
Fuel pins/assembly	201 or 264	63	217
<b>Core Parameters</b>			
Number of fuel assemblies	193	740	394
Total amount of fuel	98 000 kg	150 000 kg	25 000 kg
Core diameter	340 cm	366 cm	222 cm
Core active length	366 cm	376 cm	91 cm
Plant efficiency	33%	34%	39%
Design fuel burnup	33 GWd/tU	28 GWd/tU	100 GWd/tU
Refueling cycle	1/3 fuel/yr	1/4 fuel/yr	1/3 fuel/yr

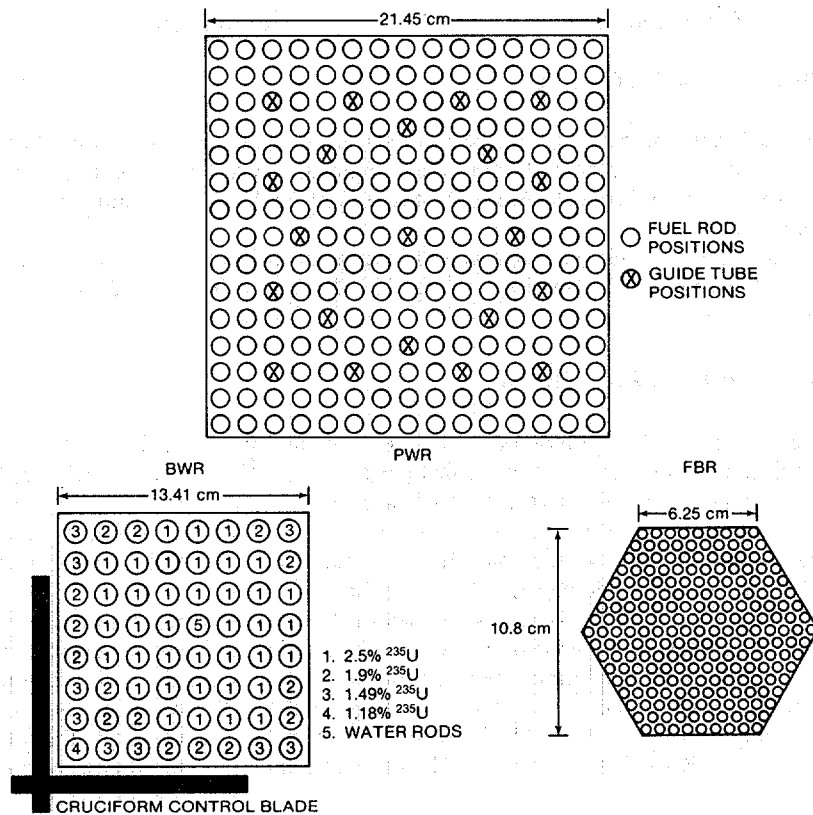


Fig. 18.1 Cross-sectional views of PWR (top), BWR (bottom left), and FBR (bottom right) fuel assemblies.

When irradiated fuel rods are chopped and leached during reprocessing, baskets of leached hulls are generated. The remaining fissile material in the leached hulls constitutes a kind of irradiated fuel. Measurement of this material is important for good process accountability (Ref. 4).

### 18.2.2 Definition of Burnup and Exposure

Two common terms for fuel irradiation, burnup and exposure, are often used interchangeably. Burnup (in atom percent) is defined as the number of fissions per 100 heavy nuclei (uranium or plutonium) initially present in the fuel. Exposure is defined as the integrated energy released by fission of the heavy nuclides initially present in the fuel. Exposure has dimensions of megawatt or gigawatt days (thermal output of the reactor) per metric ton (1000 kg) of initial uranium: MWd/tU or GWd/tU. For nondestructive measurements of irradiated fuel, the latter definition is more useful because the actual content of heavy nuclides is not directly determined.

The two definitions are approximately related by the following equation:

$$1 \text{ at \% burnup} \approx 9.6 \text{ GWd/tU} \quad (18-1)$$

The relationship between burnup and exposure changes as a function of burnup because of the changing ratio of uranium to plutonium fissions. The amount of energy released by the fission of plutonium (212 MeV) is about 5% more than the amount released by  $^{235}\text{U}$  (202 MeV).

Table 18-1 includes average design values for reactor fuel burnup. Actual values can range up to 55 to 60 GWd/tU for PWRs, 45 to 50 GWd/tU for BWRs, and 150 GWd/tU for FBRs.

### 18.2.3 Fission Product Yields

In fission reactions the primary sources of energy are the fissioning of  $^{235}\text{U}$ ,  $^{239}\text{Pu}$ , and  $^{241}\text{Pu}$ , with some contribution from the fast fissioning of  $^{238}\text{U}$ . Table 18-2 (Ref. 5) lists the relative number of fissions for each of these four isotopes as a function of fuel exposure for one typical case. The table shows that the plutonium isotopes begin to contribute a significant part of the total after only a few GWd/tU exposure, and above 20 GWd/tU exposure they become the dominant source of fissions.

Each fission results in the formation of two medium-mass fission products. Figure 18.2 (Refs. 6 and 7) shows the mass yield curves for the thermal neutron fission of  $^{235}\text{U}$  and  $^{239}\text{Pu}$ . The primary difference between the two curves is the slight shift to higher atomic mass number of the  $^{239}\text{Pu}$  curve with respect to the  $^{235}\text{U}$  curve. The shift can be seen in the relative fission yields of  $^{106}\text{Ru}$  from  $^{235}\text{U}$  and  $^{239}\text{Pu}$ . Fissions in  $^{239}\text{Pu}$  yield 11 times as much  $^{106}\text{Ru}$  as fissions in  $^{235}\text{U}$ . Thus a measurement of the gamma-ray output

Table 18-2. Percentage of total fissions as a function of fuel exposure for PWR fuel with an initial enrichment of 2.56%  $^{235}\text{U}$

Fuel Exposure (GWd/tU)	$^{235}\text{U}$	$^{238}\text{U}$	$^{239}\text{Pu}$	$^{241}\text{Pu}$
0	100.0	0.0	0.0	0.0
1.2	88.1	6.7	5.1	0.01
4.7	76.3	6.9	16.4	0.35
9.9	60.6	7.4	29.6	2.4
15.1	49.5	7.8	37.5	5.3
20.0	41.1	8.1	42.8	8.0
25.6	32.9	8.5	47.3	11.3
29.6	27.6	8.8	40.9	13.7
34.7	23.8	9.9	58.2	18.1
40.0	16.7	9.3	55.3	18.7
46.8	11.7	9.6	57.5	21.2

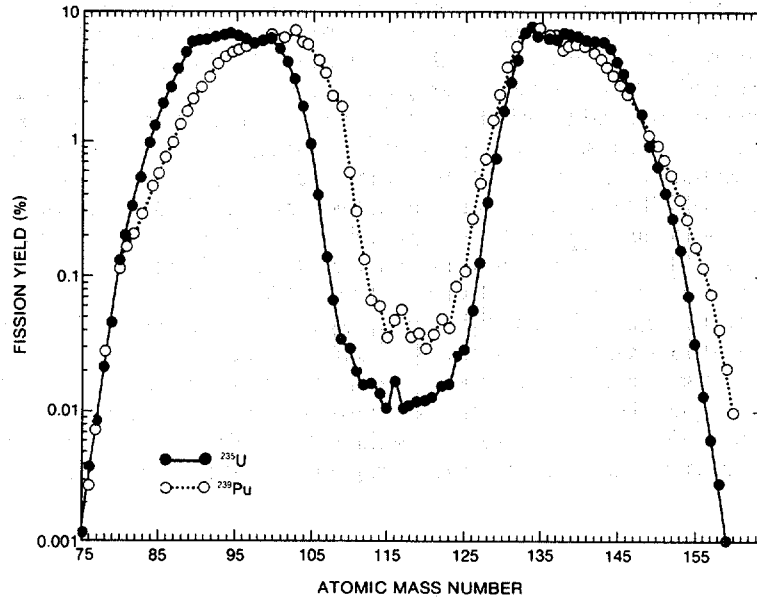


**Fig. 18.2** Mass distribution of fission products for the thermal fission of  $^{235}\text{U}$  and  $^{239}\text{Pu}$  (Refs. 6 and 7).

of  $^{106}\text{Ru}$  can determine the relative proportion of  $^{239}\text{Pu}$  fissions to total fissions. On the other hand, an isotope like  $^{137}\text{Cs}$  has nearly identical fission yields from both  $^{235}\text{U}$  and  $^{239}\text{Pu}$ . The  $^{137}\text{Cs}$  gamma-ray output can be used to determine the total number of fissions.

Most of the fission products are initially rich in neutrons and undergo beta decay to approach stability. In addition to emitting beta particles, the fission products also emit gamma rays, which result in measurable signatures. Figure 18.3 shows the gamma-ray spectrum of a PWR fuel assembly having an integral exposure of 32 GWd/tU and a cooling time of 9 months (time since discharge from the reactor). As can be seen from this spectrum, there are only about 10 isotopes that can be measured. Table 18-3 (Ref. 8) lists the most dominant isotopes, along with their gamma rays and half-lives. The fission yields are the number of nuclei of each isotope (in percent) produced on the average per thermal neutron fission in  $^{235}\text{U}$  or  $^{239}\text{Pu}$ . In addition to the fission product gamma rays, gamma rays from the activation of fuel cladding and structural materials such as  $^{54}\text{Mn}$ ,  $^{58}\text{Co}$ , and  $^{60}\text{Co}$  are also present; they are included in Table 18-3.

Uranium present in a neutron flux can also capture neutrons and build up transuranic nuclides as illustrated in Figure 18.4 (Ref. 5). Many of these nuclides produce neutrons through spontaneous fission or  $(\alpha, n)$  reactions; the spontaneous fission and  $(\alpha, n)$  neutron production rates for the primary neutron sources— $^{238}\text{Pu}$ ,  $^{240}\text{Pu}$ ,  $^{242}\text{Pu}$ ,  $^{241}\text{Am}$ ,  $^{242}\text{Cm}$ , and  $^{244}\text{Cm}$ —are included in Tables 11-1 and 11-3 in Chapter 11.

The gamma rays from fission products and the neutrons from transuranic nuclides completely mask the gamma rays and neutrons from the uranium and plutonium isotopes in the fuel. This effect is shown in Table 18-4, which lists the relative atom densities and gamma-ray output per gram of initial uranium for  $^{137}\text{Cs}$ , the 186-keV signature of  $^{235}\text{U}$ , and the 414-keV signature of  $^{239}\text{Pu}$ . These results are based on the actual irradiation history of a PWR fuel assembly. The fuel had an initial  $^{235}\text{U}$  enrichment of 2.6% and was irradiated for four reactor cycles to a maximum exposure of 46.8 GWd/tU. The fission-product and transuranic-nuclide densities were calculated using a reactor fuel depletion code (Refs. 6 and 7). Even though the atom densities for  $^{137}\text{Cs}$ ,  $^{235}\text{U}$ , and  $^{239}\text{Pu}$  are comparable at the 46.8 GWd/tU exposure level, the number of  $^{137}\text{Cs}$  gamma rays being emitted is  $4.5 \times 10^7$  and  $2.7 \times 10^7$  times the number of principal  $^{235}\text{U}$  and  $^{239}\text{Pu}$  gamma rays, respectively. The  $^{137}\text{Cs}$  isotope is just 1 of about 10 dominant gamma-emitting fission products.

Similar results are obtained when one examines the neutron output of irradiated fuel materials. Table 18-5 (Ref. 4) lists the neutron output of uranium oxide fuel after an exposure of 33.0 GWd/tU and a cooling time of 1 yr. The passive neutron yield of the plutonium is dominated by 2 orders of magnitude by the neutron yield of the curium isotopes.

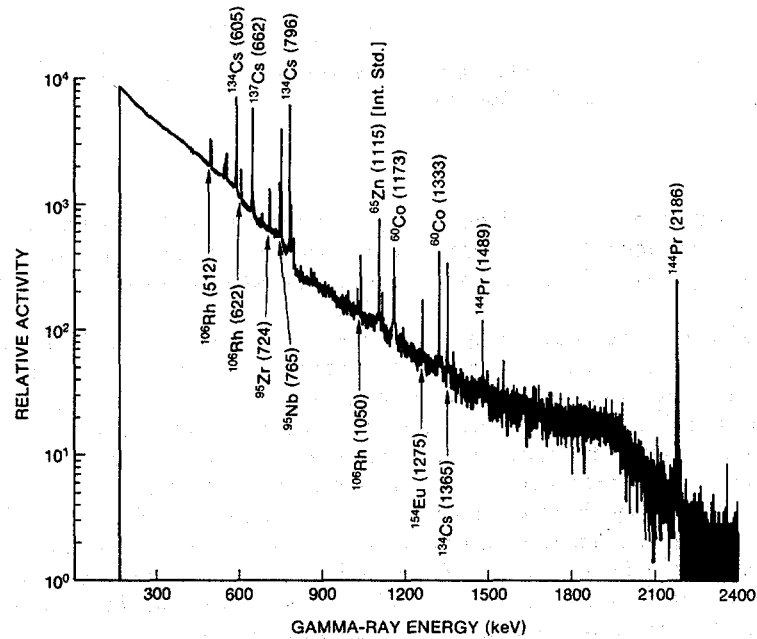


**Fig. 18.3** Gamma-ray spectrum of a PWR fuel assembly with an exposure of 32 GWd/tU and a cooling time of 9 months.

Table 18-3. Isotopes measurable by gamma rays in a typical irradiated fuel assembly (Ref. 8)

Fission Product Isotopes	Half-Life	Fission Yield in $^{235}\text{U}$ (%)	Fission Yield in $^{239}\text{Pu}$ (%)	Fission Yield Gamma-Ray Energy (keV)	Branching Ratio (%)
$^{95}\text{Zr}$	64.0 days	6.50	4.89	724.2	43.1
				756.7	54.6
$^{95}\text{Nb}$	35.0 days	6.50	4.89	765.8	99.8
$^{103}\text{Ru}$	39.4 days	3.04	6.95	497.1	86.4
				610.3	5.4
$^{106}\text{Ru-Rh}$	366.4 days	0.40	4.28	622.2	9.8
				1050.5	1.6
$^{134}\text{Cs}$	2.06 yr	$1.27 \times 10^{-5}$ a	$9.89 \times 10^{-4}$ a	604.7	97.6
				795.8	85.4
				801.8	8.7
				1167.9	1.8
				1365.1	3.0
$^{137}\text{Cs}$	30.17 yr	6.22	6.69	661.6	85.1
$^{144}\text{Ce-Pr}$	284.5 days	5.48	3.74	696.5	1.3
				1489.2	0.3
				2185.6	0.7
$^{154}\text{Eu}$	8.5 yr	$2.69 \times 10^{-6}$ a	$9.22 \times 10^{-5}$ a	996.3	10.3
				1004.8	17.4
				1274.4	35.5
<b>Activation Products</b>					
$^{54}\text{Mn}$	312.2 days			834.8	100.0
$^{58}\text{Co}$	70.3 days			811.1	99.0
$^{60}\text{Co}$	5.27 yr			1173.2	100.0
				1332.5	100.0

<sup>a</sup>Europium-154 and <sup>134</sup>Cs values are given only for direct production of the isotope from fission. Actually, each of these isotopes is produced primarily through neutron absorption. For PWR fuel material irradiated to 25 GWd/tU, the "accumulated fission yields" of <sup>154</sup>Eu and <sup>134</sup>Cs were calculated as 0.15% and 0.46%, respectively.

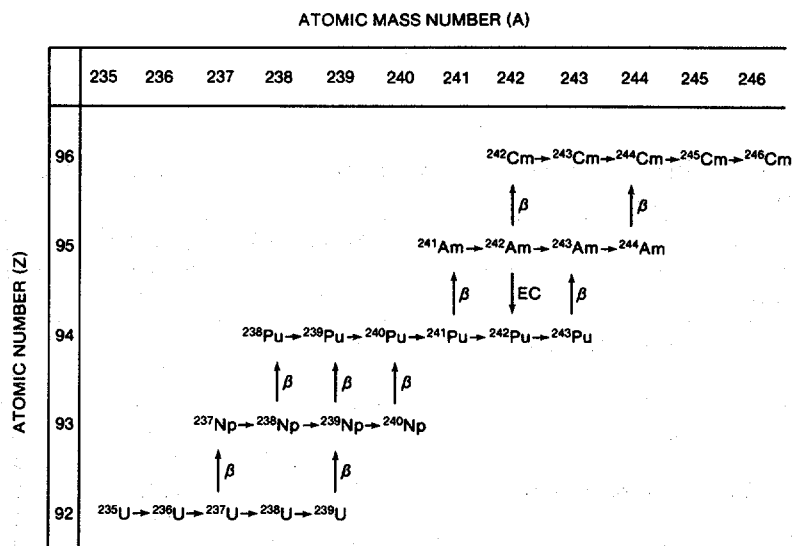


**Fig. 18.4** Principal neutron capture reactions (horizontal arrows) and beta decay reactions (vertical arrows) leading to the formation of transuranic nuclides in irradiated fuel. Both stable and metastable states exist for  $^{240}\text{Np}$ ,  $^{242}\text{Am}$ , and  $^{244}\text{Am}$ .

**Table 18-4.** Comparison of atom density and gamma-ray activity of  $^{137}\text{Cs}$  with  $^{235}\text{U}$  and  $^{239}\text{Pu}$

Fuel	$^{137}\text{Cs}$		$^{235}\text{U}$		$^{239}\text{Pu}$	
	Atom Density <sup>a</sup>	661.6 keV (gammas/g U)	Atom Density <sup>a</sup>	185.72 keV (gammas/g U)	Atom Density <sup>a</sup>	413.69 keV (gammas/g U)
0	0.0	0.0	6.28 E+19	1.06 E+03	0.0	0.0
1.2	1.94 E+17	1.20 E+08	5.94 E+19	1.00 E+03	1.66 E+18	2.28 E+01
4.7	7.63 E+17	4.73 E+08	5.05 E+19	8.51 E+02	5.39 E+18	7.41 E+01
9.9	1.60 E+18	9.94 E+08	3.98 E+19	6.70 E+02	8.74 E+18	1.20 E+02
15.1	2.43 E+18	1.51 E+09	3.12 E+19	5.25 E+02	1.05 E+19	1.44 E+02
20.0	3.17 E+18	1.97 E+09	2.47 E+19	4.16 E+02	1.14 E+19	1.57 E+02
25.6	4.05 E+18	2.51 E+09	1.87 E+19	3.14 E+02	1.19 E+19	1.64 E+02
29.6	4.64 E+18	2.87 E+09	1.52 E+19	2.56 E+02	1.20 E+19	1.65 E+02
34.7	5.40 E+18	3.35 E+09	1.15 E+19	1.94 E+02	1.20 E+19	1.65 E+02
40.0	6.15 E+18	3.81 E+09	8.59 E+18	1.45 E+02	1.20 E+19	1.65 E+02
46.8	7.14 E+18	4.43 E+09	5.80 E+18	9.78 E+01	1.18 E+19	1.62 E+02

<sup>a</sup>Number of atoms per gram of initial heavy metal.



Table 18-5. Typical neutron production from oxide fuel

Nuclide	g/tU	n(SF)/s-tU	n( $\alpha$ ,n)/s-tU
<sup>238</sup> Pu	$1.35 \times 10^2$	$3.67 \times 10^5$	$2.48 \times 10^6$
<sup>240</sup> Pu	$2.32 \times 10^3$	$2.02 \times 10^6$	$4.66 \times 10^5$
<sup>242</sup> Pu	$4.61 \times 10^2$	$8.16 \times 10^5$	
<sup>241</sup> Am	$8.83 \times 10^1$		$3.21 \times 10^5$
<sup>242</sup> Cm	2.43	$5.44 \times 10^7$	$1.15 \times 10^7$
<sup>244</sup> Cm	18.3	$2.07 \times 10^8$	$1.88 \times 10^6$
		$2.65 \times 10^8$	$1.66 \times 10^7$

### 18.3 INDIRECT SIGNATURES FOR FUEL BURNUP

As described in Section 18.2.3, passive neutron or gamma-ray assay of irradiated fuel cannot directly measure fissile element content or fuel burnup because of the high ambient radiation levels. This section describes a variety of indirect techniques for qualitative or quantitative determination of fuel burnup, most of which exploit these high ambient radiation levels.

#### 18.3.1 Physical Attributes

Before determining burnup, an inspector can identify the irradiated fuel assemblies and verify their mass. The fuel assemblies are discrete units stamped with identification numbers. If the water in the storage pond is clear, the identification numbers can be read using a set of binoculars and a floating Plexiglas window to eliminate water ripples. If the water is not clear enough to permit this easy verification, an underwater periscope or TV camera (available at most reactor storage ponds) can be used. Information about the physical integrity of the fuel assembly can be obtained by using a load cell to verify the mass. Most storage ponds have a crane mechanism for moving the stored fuel assemblies, and a load cell can be mounted on the crane.

Visual inspection of a fuel assembly can usually indicate whether the assembly has been in the core. A fresh fuel assembly has a shiny surface, whereas the surface of an irradiated fuel assembly has undergone slight oxidation resulting in a dull reddish layer. Also, visible encrustation may build up on the irradiated fuel assembly, and the assembly may be slightly bent or twisted.

#### 18.3.2 Cerenkov Radiation

The gamma rays from fission and activation products produce electrons that result in the emission of Cerenkov light. Thus, measurement of Cerenkov light can be used to indicate the presence of gamma-emitting material. This indirect signature has been used to verify spent-fuel assemblies stored underwater (Refs. 9 and 10).

Electromagnetic Cerenkov radiation is emitted whenever a charged particle passes through a medium with a velocity exceeding the phase velocity of light in that medium. In water, the phase velocity of light is about 75% of the value in vacuum. Thus, for example, any electron passing through water and having at least 0.26 MeV of kinetic energy will emit Cerenkov radiation. Irradiated fuel assemblies are a prolific source of beta particles, gamma rays, and neutrons. All three types of emissions can produce Cerenkov light, directly or indirectly.

The most significant production of Cerenkov light is from high-energy fission product gamma rays that interact with the fuel cladding or storage water. This interaction produces electrons and positrons by Compton scattering and other effects. Calculations of the number of Cerenkov photons generated from these beta particles indicate that Cerenkov light production in the visible wavelength range of 4000 to 6000 Å is negligible for gamma rays with energies below 0.5 MeV, but rises steeply with higher energy. A 2-MeV gamma ray produces 500 times more Cerenkov light than a 0.6-MeV gamma ray.

The absolute Cerenkov light level and its decay with time are related to burnup. Hiding a diversion either by substitution of dummy fuel assemblies or by incorrectly stating burnup would be difficult as long as the Cerenkov light intensity can be measured accurately.

### 18.3.3 Single Fission Product Gamma-Ray Activity

The buildup of specific fission products can be used as a quantitative measure of burnup. The absolute gamma-ray activity of a particular fission product can serve as a burnup monitor if the following conditions are met (Ref. 11):

(1) The fission product should have equal fission yields for the major uranium and plutonium fissioning nuclides. If the yields are substantially different, the effective fission yield will depend somewhat on the reactor's operating history.

(2) The neutron capture cross section of the fission product must be low enough so that the observed fission product concentration is due only to heavy element fission and not to secondary neutron capture reactions.

(3) The fission product half-life should be long compared to the fuel irradiation time, so that the quantity of fission product present is approximately proportional to the number of fissions.

(4) The fission product gamma rays must be relatively high energy (500 keV or more) to escape from the fuel pin. For a 1-cm-diam oxide fuel pin, 39% of the 662-keV  $^{137}\text{Cs}$  activity is absorbed within the pin. This strong self-absorption implies that, in practice, passive gamma-ray measurements of fuel assemblies are limited to the outer rows. A further complication is that a nonuniform neutron flux during irradiation can lead to nonuniform burnup within the assembly. This is particularly true for BWR fuel assemblies because two sides of each assembly are adjacent to control blades.

If the above conditions are satisfied, the measured gamma-ray activity  $I$  (counts/s) from the fission product is proportional to the number  $N$  of fission product nuclei formed during irradiation:

$$I = \epsilon k S N \lambda e^{-\lambda T} \quad (18-2)$$

where  $\varepsilon$  = absolute detector efficiency  
 $k$  = branching ratio  
 $S$  = attenuation correction  
 $\lambda$  = fission product decay rate  
 $T$  = cooling time.

After solving Equation 18-2 for  $N$ , the fuel burnup can be calculated from the equation

$$\text{at \% burnup} = 100 \times (N/Y)/U \quad (18-3)$$

where  $Y$  = effective fission product yield  
 $U$  = number of initial uranium atoms.

Cesium-137 is the most widely accepted indicator of fuel burnup because its neutron absorption cross sections are negligible, its yields from both  $^{235}\text{U}$  and  $^{239}\text{Pu}$  are approximately the same, and its 30-yr half-life makes a correction for reactor power history unnecessary (Ref. 11). Figure 18.5 shows the calculated buildup of  $^{137}\text{Cs}$  for the 46.8 GWd/tU exposure PWR fuel assembly described in Section 18.2.3. The  $^{137}\text{Cs}$  buildup is approximately linear over the entire range of burnup. A comparison of measured  $^{137}\text{Cs}$  activity with burnup is given in Section 18.4.3. Past experience with the  $^{137}\text{Cs}$  burnup monitor shows that the absolute  $^{137}\text{Cs}$  activity can determine burnup to an accuracy of 1 to 4% for individual fuel rods.

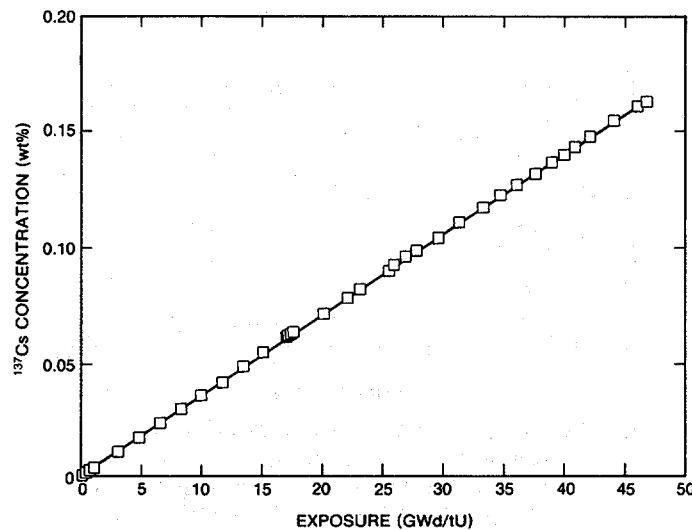


**Fig. 18.5** Calculated dependence of the  $^{137}\text{Cs}$  fission product concentration, expressed as a percentage of the initial uranium concentration, on exposure for the 46.8 GWd/tU exposure PWR fuel assembly described in Section 18.2.3.

For gamma-ray measurements of leached hulls, the 2186-keV line of  $^{144}\text{Ce-Pr}$  is preferred to the 662-keV line of  $^{137}\text{Cs}$  because of its greater penetrability and because  $^{144}\text{Ce-Pr}$  is less susceptible to leaching during fuel dissolution.

### 18.3.4 Total Gamma-Ray Activity

The total gamma-ray activity of irradiated fuel is the sum of the activities from each fission product and transuranic element, with each activity given by an equation like Equation 18-2. Most of the gamma-ray activity comes from a few important fission products. The contribution of each of these fission products to the total activity varies with cooling time, as illustrated in the example given in Figure 18.6. For cooling times greater than 1 yr, the total gamma-ray activity is roughly proportional to burnup. For shorter cooling times, this relationship does not hold because the total gamma-ray activity is dominated by the buildup and decay of short-lived fission products like  $^{95}\text{Nb}$  and  $^{95}\text{Zr}$ . The concentrations of these isotopes depend, in part, on the reactor operating history and the proximity of reactor control materials. After longer cooling times, the short-lived isotopes have decayed and the detector response is dominated by long-lived isotopes that are less dependent on operating history and other factors.

A rapid way to determine the consistency of operator-declared values for burnup and cooling time has been developed using total gamma-ray activity (Refs. 12 and 13). The total activity is divided by the declared burnup and is plotted as a function of the declared cooling times. The result is a relationship of the form  $aT^b$ , where  $a$  and  $b$  are scaling parameters and  $T$  is the cooling time. An example of this relationship for PWR fuel assemblies is given in Figure 18.7. The shape of the curve is due primarily to the half-lives of  $^{134}\text{Cs}$  and  $^{137}\text{Cs}$ .

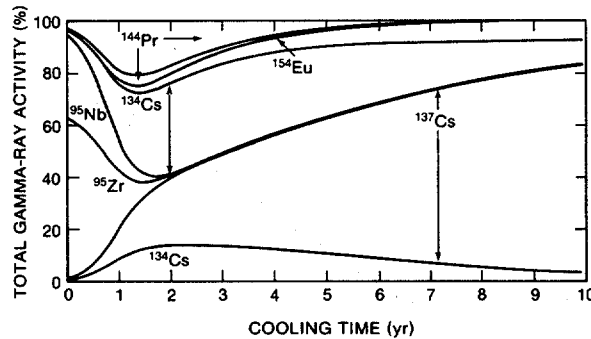


**Fig. 18.6** An example of the variation in fission product gamma-ray activity as a function of cooling time, with each major gamma ray given as a percentage of the total activity. Note that  $^{144}\text{Pr}$  and  $^{134}\text{Cs}$  each have two major gamma rays shown. The curves are based on measurements of a PWR fuel assembly with an exposure of 12.18 GWd/tU and a cooling time of 2 yr. The extrapolation to longer and shorter cooling times was done by calculation.

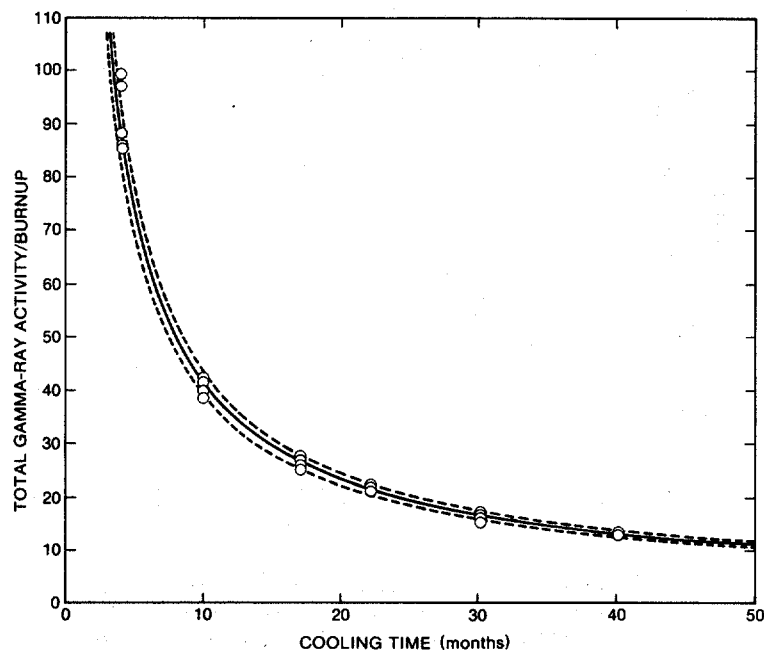


**Fig. 18.7** Measured total gamma-ray activity divided by burnup as a function of cooling time for PWR fuel assemblies. The fitted curve illustrates how the total gamma-ray activity can be used to verify the consistency of operator-declared values for burnup and cooling time.

### 18.3.5 Fission Product Activity Ratios

The burnup of irradiated fuel can also be determined from the ratios of some fission product isotopes. The isotopic ratios can be determined from gamma-ray activity ratios using equations like Equation 18-2. The two most commonly used isotopic ratios are  $^{134}\text{Cs}/^{137}\text{Cs}$  and  $^{154}\text{Eu}/^{137}\text{Cs}$ .

Cesium-134 is produced by neutron capture on the fission product  $^{133}\text{Cs}$ ; therefore, its production requires two neutron interactions. The first is the neutron that causes fission of the uranium or plutonium, and the second is the  $^{133}\text{Cs}(n,\gamma)$  reaction. Because these interactions are the primary source of  $^{134}\text{Cs}$ , the concentration of  $^{134}\text{Cs}$  within the fuel is approximately proportional to the square of the integrated flux. By dividing the concentration of  $^{134}\text{Cs}$  by the concentration of  $^{137}\text{Cs}$ , which is directly proportional to the integrated flux, the ratio becomes approximately proportional to the burnup (total flux). This is a simplified explanation in that there are other factors such as the spectral dependence of the  $(n,\gamma)$  cross section that must be considered in a more rigorous derivation. However, in practice, the  $^{134}\text{Cs}/^{137}\text{Cs}$  isotopic ratio has worked well for determining the burnup of both light-water-reactor and fast-breeder-reactor fuel materials (Refs. 14 and 15). The  $^{154}\text{Eu}/^{137}\text{Cs}$  isotopic ratio also has a fairly linear dependence on exposure (Refs. 8 and 16).

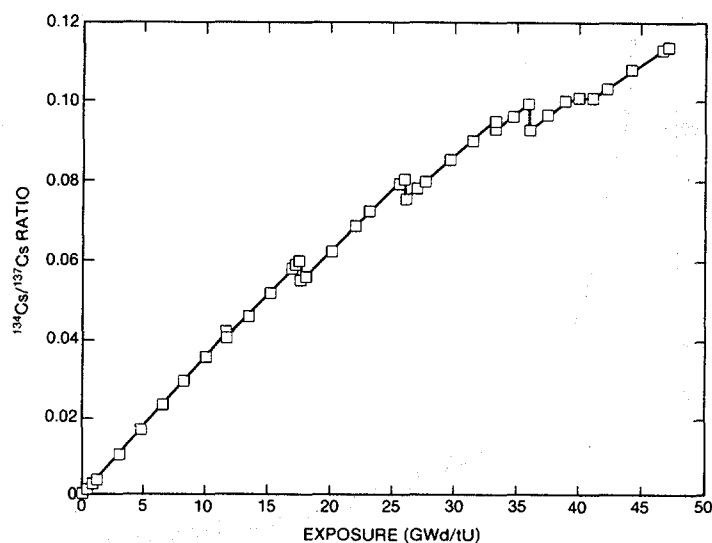


**Fig. 18.8** Calculated dependence of the  $^{134}\text{Cs}/^{137}\text{Cs}$  isotopic ratio on exposure for the PWR fuel assembly described in Section 18.2.3. Discontinuities in the curve are due to discontinuities in the reactor operating history.

Figure 18.8 shows the calculated  $^{134}\text{Cs}/^{137}\text{Cs}$  isotopic ratio as a function of exposure for the 46.8 GWd/tU PWR fuel assembly described in Section 18.2.3. The discontinuities in the curve of Figure 18.8 are due to discontinuities in the reactor operating history, which emphasizes the fact that the use of isotopic ratios requires correcting for the decay of the isotopes. This correction is important for the  $^{134}\text{Cs}/^{137}\text{Cs}$  ratio because of the 2.06-yr half-life of  $^{134}\text{Cs}$ . For the  $^{154}\text{Eu}/^{137}\text{Cs}$  isotopic ratio the 8.5-yr half-life of  $^{154}\text{Eu}$  and the 30.2-yr half-life of  $^{137}\text{Cs}$  make the correction less important. In general, calibration curves are computed to the time of discharge to eliminate the effects of the different decay rates of the fission products. Several techniques have been suggested to obtain cooling time corrections by examining certain isotopic ratios (Refs. 13 and 16 through 18).

For field measurements, fission product activity ratios are easier to determine than absolute activities because only relative detector efficiencies must be known. However, it is still necessary to correct for changes in detection efficiency with gamma-ray energy. The  $^{134}\text{Cs}$ ,  $^{137}\text{Cs}$ , and  $^{154}\text{Eu}$  gamma rays have different energies and therefore different detection efficiencies. A relative efficiency calibration can be performed using multiple gamma rays from  $^{134}\text{Cs}$  and  $^{154}\text{Eu}$ ; the procedure is identical to that described in Section 8.4.1 of Chapter 8 for determining the relative efficiency curve for plutonium isotopic composition measurements. This allows one to obtain the relative detection efficiency of the corresponding gamma rays using only the original gamma-ray spectra.

### 18.3.6 Total Neutron Output

The total neutron output of irradiated fuel can also serve as an indicator of burnup, and has both advantages and disadvantages relative to the gamma-ray output. The neutron signal comes only from the fuel, not from the cladding materials. Attenuation of the neutron signal within the fuel assembly is less than attenuation of the gamma-ray signal; in fact, induced fissions within the assembly result in nearly equal response from both interior and exterior fuel pins. The neutron measurements can be made soon after the fuel is discharged from the reactor, while the gamma-ray signal is still dominated by the decay of short-lived isotopes that reflect recent reactor power levels. A disadvantage of the neutron signal is that the quantity of primary neutron emitting isotopes is only indirectly correlated to exposure. Also, in principle, neutron detectors are sensitive to gamma rays, although the fission chambers used for measurements today are almost completely insensitive to gamma rays.

The five principal neutron sources in a PWR fuel assembly with a typical exposure of 31.5 GWd/tU are plotted in Figure 18.9 as a function of cooling time. For other fuel assemblies or different burnup levels,  $^{241}\text{Am}$  or  $^{246}\text{Cm}$  may also be significant neutron sources. However,  $^{244}\text{Cm}$  and  $^{242}\text{Cm}$  are usually the two dominant neutron-emitting isotopes. Because of the short half-lives of these two isotopes (18.1 and 0.45 yr, respectively), the cooling time of the fuel must be known to interpret correctly the total neutron output. Operator-declared values for the cooling time can be verified by measuring the total gamma-ray activity, as described in Section 18.3.4.

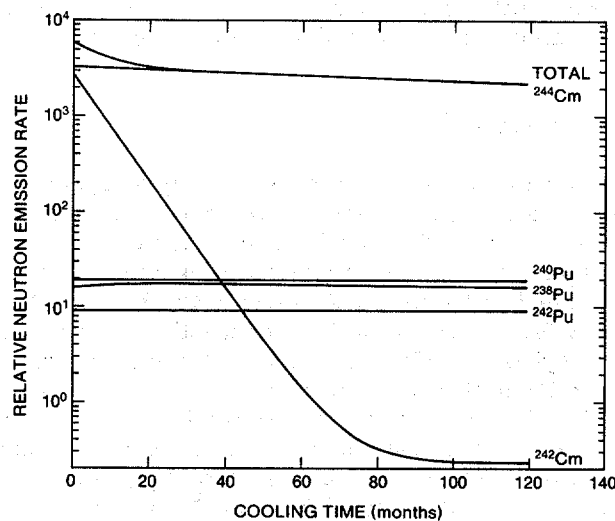


**Fig. 18.9** The five principal neutron sources in a PWR fuel assembly with an exposure of 31.5 GWd/tU. At long cooling times, the decay of  $^{242}\text{Cm}$  follows the decay of its parent,  $^{242m}\text{Am}$ , a metastable state of  $^{242}\text{Am}$  with a half-life of 153 years.

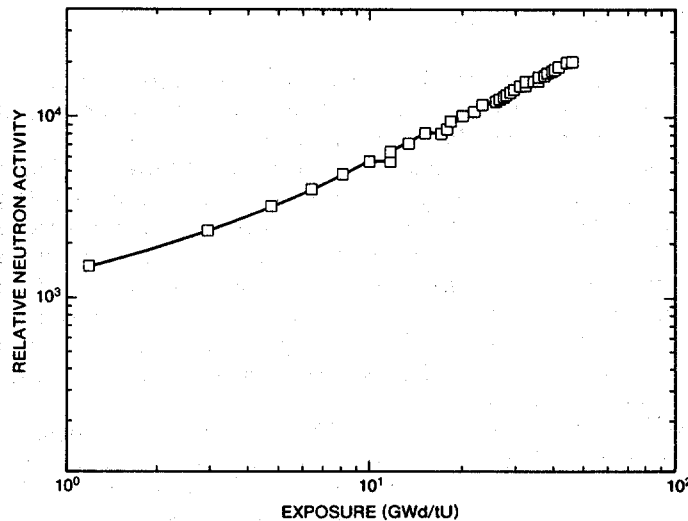


*Fig. 18.10* Calculated dependence of total neutron output on exposure for the PWR fuel assembly described in Section 18.2.3.

Figure 18.10 shows the calculated relationship between the total neutron output and exposure for the PWR fuel assembly described in Section 18.2.3. Above 10 GWd/tU exposure, the relationship can be approximated by the following empirical power function:

$$\text{neutron rate} = \alpha (\text{exposure})^\beta \quad (18-4)$$

Equation 18-4 has been demonstrated for a wide variety of light-water-reactor fuels (Refs. 19 through 22), and makes it possible to determine burnup from the observed total neutron output. The value of  $\beta$  is usually between 3.0 and 4.0.

The rate of buildup of the principal neutron-emitting transuranic isotopes is relatively insensitive to the initial fuel density and power levels; however, the initial  $^{235}\text{U}$  enrichment and the fuel irradiation history can significantly influence the rate of buildup. Figure 18.11 shows the effect that initial  $^{235}\text{U}$  enrichment has on the neutron emission rate. [The effects of attenuation and multiplication have not been incorporated into these values.] For identical exposures the lower-enriched fuel has a higher neutron emission rate. Lower-enriched fuel has less fissile material per unit volume and therefore requires a higher neutron fluence to achieve the same burnup as a higher-enriched fuel. The higher neutron fluence results in more  $^{242}\text{Cm}$  and  $^{244}\text{Cm}$  buildup and a correspondingly higher neutron emission rate.

Noncontinuous irradiation histories can also have a significant effect upon the neutron emission rate as is evidenced by the curves presented in Figure 18.12. The effect of noncontinuous irradiation history is short-term, due primarily to the increased buildup of  $^{242}\text{Cm}$  following any period of cooling time. During any nonirradiation



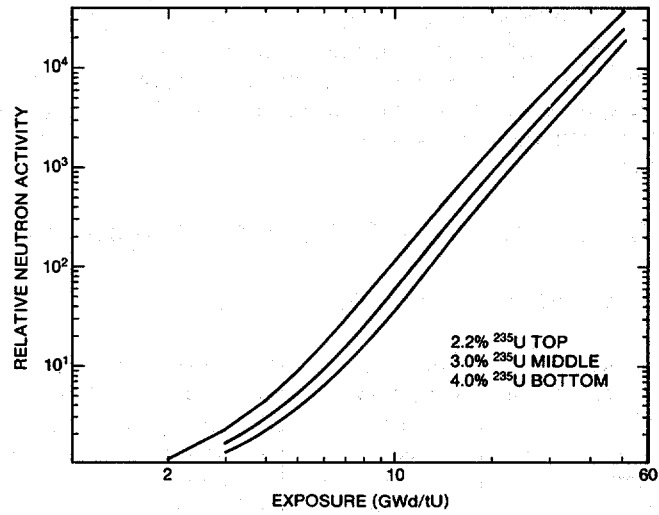


**Fig. 18.11** Calculated dependence of total neutron output on initial fuel enrichment for identical exposure values. The calculations are based on the PWR fuel assembly described in Section 18.2.3.

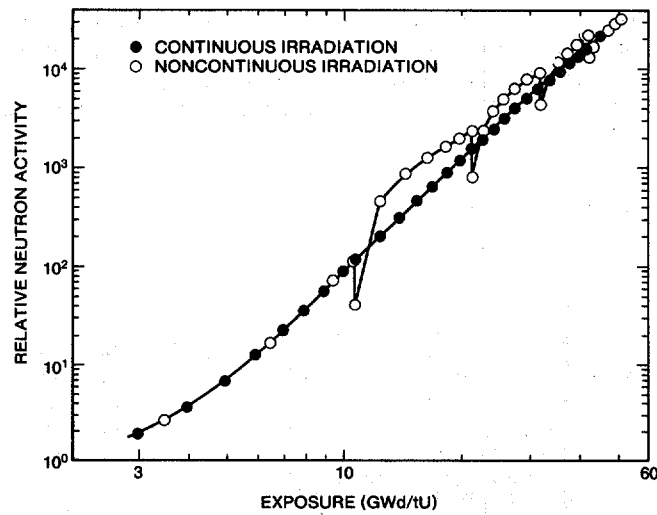


**Fig. 18.12** Calculated dependence of total neutron output on reactor operating history for the PWR fuel assembly described in Section 18.2.3. A continuous 5-yr irradiation history (closed circles) is compared with a discontinuous history of alternating years of operation and cooling (open circles).

period,  $^{241}\text{Pu}$  ( $t_{1/2} = 14.35$  yr) decays to form  $^{241}\text{Am}$  ( $t_{1/2} = 433.6$  yr). When this material is reinserted into a high-neutron flux, large amounts of  $^{242}\text{Cm}$  form through neutron capture in  $^{241}\text{Am}$ . If the fuel were measured after a longer cooling time ( $\sim 2$  yr), most of the  $^{242}\text{Cm}$  would have decayed, and the measured neutron emission rates would be more consistent with the rates obtained from fuel material that had undergone continuous irradiation.

## 18.4 GAMMA-RAY MEASUREMENT OF IRRADIATED FUEL

### 18.4.1 Total Gamma-Ray Activity Measurements

The total gamma-ray activity of submerged fuel assemblies can be measured with ion chambers, scintillators, or thermoluminescent dosimeters (TLDs). Ion chambers and scintillators provide a direct readout with only 1 to 2 min required for positioning the detectors and collecting the data. Thermoluminescent dosimeters must be removed from the water and read out with special instrumentation. Figure 18.13 illustrates a geometry used for gamma-ray measurements of irradiated fuel assemblies and shows an ion chamber placed adjacent to the top of a fuel assembly.

When the total gamma-ray activity is measured at the top of the fuel assembly, the response is due primarily to  $^{60}\text{Co}$ ,  $^{58}\text{Co}$ , and  $^{54}\text{Mn}$  activation products in the structural material. When the fuel assembly is raised above the storage rack, but still submerged, total gamma-ray-activity measurements can be made alongside the assembly. Then the response is due primarily to fission products in the fuel rods. Under these conditions, the consistency of operator-declared values for cooling time and burnup has been verified to an accuracy of about 10%. Fuel assemblies with unusual irradiation histories have been identified easily. An ion chamber designed to be placed against the side of a fuel assembly has been incorporated into the fork detector described in Section 18.5.

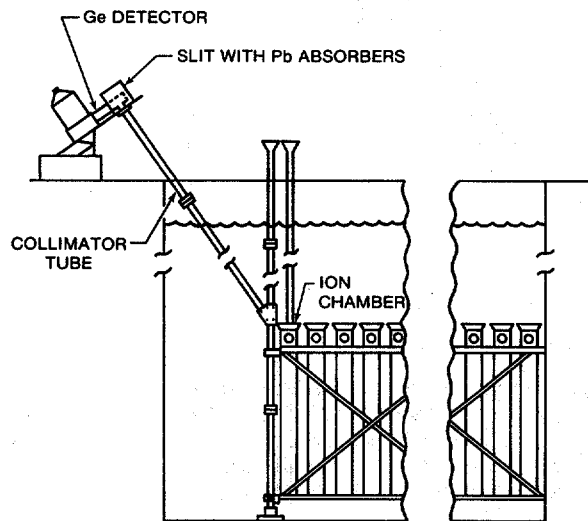


**Fig. 18.13** Gamma-ray measurements of irradiated fuel in a storage pond. The figure shows a high-resolution germanium detector with its collimator tube and an ion chamber installed at the top of a storage rack. The fuel assembly is raised vertically for measurement.

### 18.4.2 High-Energy Gamma-Ray Activity Measurements

A more specific gamma-ray measurement can be made with a Be( $\gamma$ ,n) detector. Such a detector consists of a  $^{235}\text{U}$  fission chamber surrounded by polyethylene, which is in turn surrounded by beryllium. Neutrons produced by a photoneutron reaction in the beryllium are thermalized in the polyethylene and detected by the fission chamber. Because the threshold for photoneutron production in beryllium is 1665 keV, the only significant fission product signature observed by this detector is the 2186-keV gamma ray from  $^{144}\text{Ce-Pr}$ .

If the Be( $\gamma$ ,n) detector is placed alongside irradiated-fuel materials, it will measure relative  $^{144}\text{Ce-Pr}$  fission product activity and will be insensitive to lower-energy activation products. Like other gamma-ray detectors, this detector is not useful at the top of an irradiated fuel assembly because the gamma rays are shielded by structural materials. Neutrons emitted by the fuel or produced by (n,2n) reactions in the beryllium can interfere with the photoneutron measurement if their numbers are significant.

### 18.4.3 High-Resolution Gamma-Ray Spectroscopy

More detailed information on fuel burnup can be obtained by high-resolution gamma-ray spectroscopy. The concentration of individual fission products can be determined by measuring single fission product gamma-ray activities; these isotopic concentrations can be related to fuel burnup (see Section 18.3.3). Also, some gamma-ray activity ratios can be used to calculate fission product isotopic ratios that can be related to burnup (see Section 18.3.5).

The objective of high-resolution measurements is to obtain gamma-ray spectra that accurately represent the fission- and activation-product inventory of the entire fuel assembly. The instrumentation required to perform these measurements is more complex than that required for total gamma-ray activity measurements or Cerenkov glow measurements. A germanium detector with a standard high-resolution amplifier and a multichannel analyzer is required to collect and analyze the spectra. Some type of magnetic storage medium is highly desirable for recording the data. The germanium detector views the submerged fuel assembly through a long, air-filled collimator (with a minimum length of 3 m for radiation shielding), as illustrated in Figure 18.13. Individual fuel assemblies must be moved to the scanning system by the facility operator for measurement.

The air-filled collimator defines the volume segment of the fuel assembly from which the gamma-ray spectrum is collected. Because of its length, the collimator reduces the dose rate at the detector to an acceptable level. The maximum dose rate obtained with a 5-cm-diam, 6-m-long collimator from 40-GWd/tU exposure fuel with a 2-yr cooling time is only about 10 mR/h. Usually the background radiation level is in approximately the same range. The germanium detector must be shielded from the background radiation; otherwise, the detector will not be sensitive to the gamma rays from the fuel assembly. Also, thin pieces of lead, copper, and cadmium may be placed in front of the detector to reduce the source intensity from the fuel assembly.

---

The self-attenuation of the fuel material can significantly influence the measured signals. For example, as discussed in Section 18.3.5, the isotopic ratio  $^{154}\text{Eu}/^{137}\text{Cs}$  can be used to determine the burnup of fuel assemblies. Nearly 92% of the measured  $^{137}\text{Cs}$  signature (661.6 keV) originates in the three outer rows of fuel pins in a PWR fuel assembly (Ref. 23). However, because only 78% of the  $^{154}\text{Eu}$  signature (1275 keV) originates in these three outer rows, the ratio  $^{154}\text{Eu}/^{137}\text{Cs}$  does not sample exactly the same volume segment of the fuel assembly.

The data analysis for high-resolution measurements is not difficult when only relative values are needed. The net areas for  $^{137}\text{Cs}$ ,  $^{134}\text{Cs}$ , and  $^{154}\text{Eu}$  can be obtained from the multichannel analyzer; the isotopic concentrations and isotopic ratios can be obtained using Equation 18-2. For isotopic ratios, the relative efficiency corrections can be obtained by using a relative efficiency calibration, as described in Section 18.3.5 (Refs. 24 through 26). This technique corrects for differences in the self-attenuation of the source materials, the detector efficiency, and the scanning geometry. Also, standard analysis techniques generally require correction for isotopic decay to the time of discharge from the reactor or some other specified time. The  $^{137}\text{Cs}$  concentration and the  $^{134}\text{Cs}/^{137}\text{Cs}$  and  $^{154}\text{Eu}/^{137}\text{Cs}$  isotopic ratios can then be plotted for a set of fuel assemblies to obtain the relative burnups. If one destructive analysis of the fuel is available, absolute values for the burnups can be calculated.

Many reports (for example, Refs. 16 and 27) describe the use of gamma rays to characterize irradiated fuel materials. Two such applications are given in Figures 18.14 and 18.15, which compare the  $^{137}\text{Cs}$  activity and the  $^{134}\text{Cs}/^{137}\text{Cs}$  isotopic ratio with burnup for 14 PWR fuel assemblies with exposures of 16 to 33 GWd/tU. Each data set was analyzed using regression analysis to obtain the linear relationship. The other two lines on each plot represent the 95% confidence limits that a subsequent measurement would fall within these limits. The average differences between the regression line and the measured data points were 4.9% for  $^{137}\text{Cs}$  and 4.6% for  $^{134}\text{Cs}/^{137}\text{Cs}$ . Similar numbers in the range of 4 to 8% can be obtained under most measurement conditions.

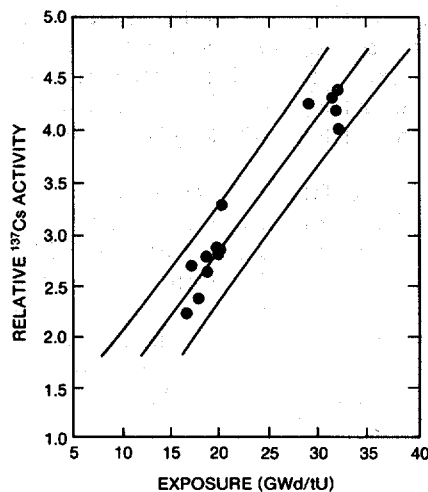


**Fig. 18.14** Correlation of the measured  $^{137}\text{Cs}$  activity (arbitrary units) with declared exposure for 14 PWR assemblies (Ref. 16).

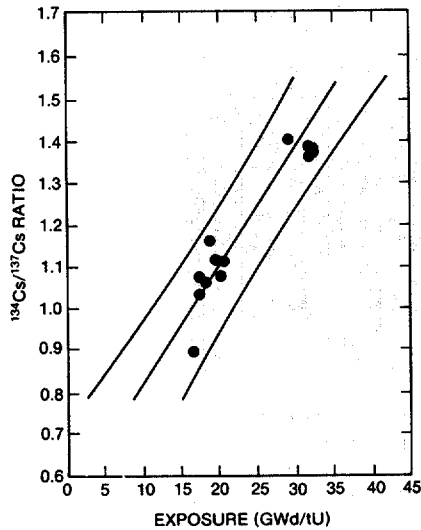


Fig. 18.15 Correlation of the measured  $^{134}\text{Cs}/^{137}\text{Cs}$  isotopic ratio with declared exposure for 14 PWR assemblies (Ref. 16).

#### 18.4.4 Cerenkov Radiation Measurements

The Cerenkov glow measurement provides a rapid nondestructive technique for verifying the presence of a gamma-ray source distributed within the fuel assembly. It can also be used to determine the absence of fuel pins in a fuel assembly. The fuel assemblies can be verified without placing any instrumentation into the storage pond water. However, most of the artificial lighting has to be eliminated, which the facility operator may not allow. When the artificial lighting can be eliminated, the inspector must move around in a darkened environment to carry out the measurements. Thus, the Cerenkov instrument should (1) be lightweight and easy to position by hand, (2) give an immediate result, (3) be insensitive to radiation damage, and (4) have an accuracy ensuring a meaningful measurement of the fuel inventory.

Figure 18.16 shows an instrument that is capable of both viewing the Cerenkov glow emitted and also determining the intensity of the glow (Ref. 10). The instrument is composed of two basic components: an image-amplifying portion and an electro-optical package that uses a photomultiplier tube to measure the intensity of the light passing through the aperture and field lens. The photomultiplier tube output current provides a digital readout indication of the intensity of the incoming light. Calibration of the instrument is done using a carbon-14 phosphor light source built into a special lens cap.

The light intensity profile is very sharp as the instrument is scanned horizontally across the top of an assembly because of the highly collimated nature of the emitted Cerenkov light. For fuel stored in standard vertical assemblies, penetrations in the top plates and tie plates and interstices between the fuel pins serve as Cerenkov light channels. These channels allow radiation from the entire length of the fuel assembly to be sampled by viewing from above. A series of measurements have been performed at storage facilities to demonstrate the usefulness of the technique for rapid verification of

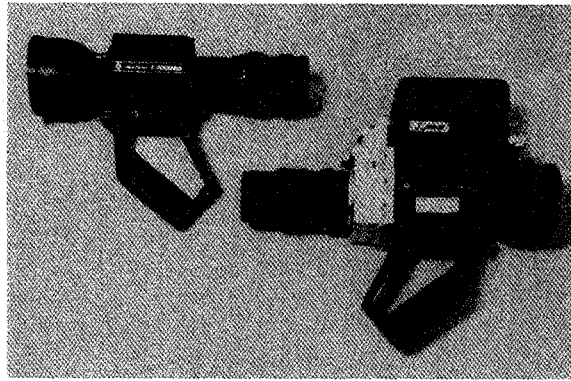


**Fig. 18.16** Hand-held instrument for viewing the Cerenkov glow from irradiated fuel and determining its intensity. The instrument (shown on the right) is an adaptation of a commercially available night-vision device (shown on the left).

irradiated fuel assemblies (Ref. 10). Figure 18.17 shows the Cerenkov image of two PWR fuel assemblies in a storage rack at a reactor storage pond. The bright spots correspond to the guide tube positions of a  $15 \times 15$  fuel assembly. Adjacent fuel assemblies do not exhibit similar sets of bright spots because the observer is not aligned with the axes of the assemblies.

The Cerenkov glow measurements are less susceptible to crosstalk among adjacent assemblies than are gamma-ray intensity measurements made at the top of the assemblies (Ref. 28). This is because Cerenkov light is channeled up from the entire length of the assembly, whereas gamma-ray measurements made at the top are mainly due to activation of the structural components. The spatial extent of the Cerenkov glow surrounding an isolated irradiated assembly in water is determined by the gamma radiation from the assembly's outer pins. The thickness of water required to reduce the intensity of 1-MeV gamma rays to one-tenth is  $\sim 36$  cm, which is a reasonable estimate of the Cerenkov "halo" around an isolated point source. Fission product radiation from an assembly's inner pins, however, must penetrate a much denser composite of fuel cladding and interstitial water, which greatly reduces crosstalk.

## 18.5 NEUTRON MEASUREMENT OF IRRADIATED FUEL

Neutron measurements of irradiated fuel are relatively easy to make and can provide a rapid indication of burnup. The detection equipment is simple and easy to operate and a preliminary analysis of the data can be performed at the facility. A neutron detector is placed adjacent to the fuel assembly and the signal is analyzed using a single-channel analyzer. A  $^{235}\text{U}$  fission chamber is the preferred detector because of its insensitivity to gamma rays. Although neutrons can penetrate the fuel assembly more readily than gamma rays can, their attenuation in water is more severe. The gamma-ray signal

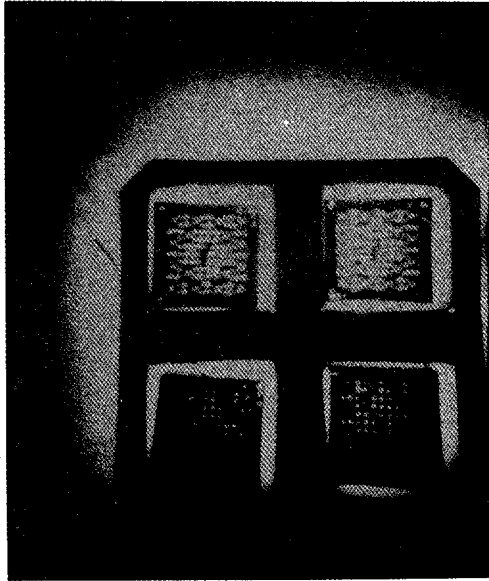


*Fig. 18.17 Cerenkov glow image of two PWR fuel assemblies in a reactor storage pond.*

decreases by a factor of 10 in roughly 36 cm, whereas the neutron signal decreases by a factor of 10 in about 10 cm. Thus it is important to position the neutron detector close to the fuel assembly.

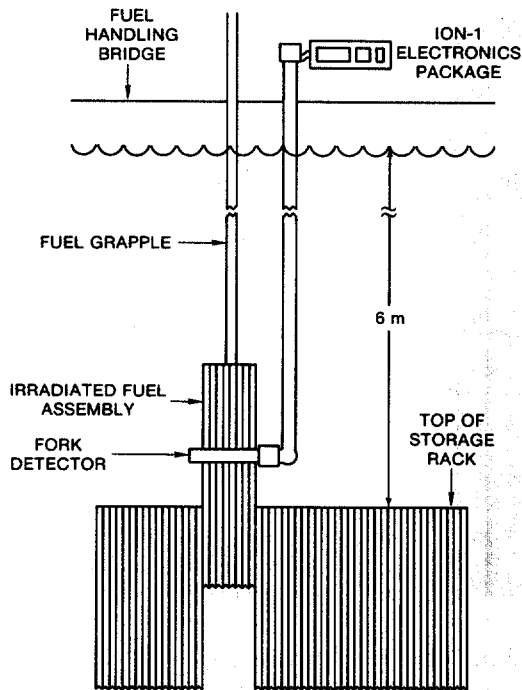
#### **18.5.1 The Fork Detector and ION-1 Electronics Package**

Figure 18.18 illustrates a neutron measuring system developed for use by safeguards inspectors (Refs. 29 and 30). The system is designed to measure the total neutron and total gamma-ray activity of a submerged fuel assembly. The two principal components, a fork detector and an ION-1 electronics package, are shown in Figure 18.19.

The fork detector is a watertight polyethylene detector head containing two sets of ion chambers and fission chambers for measuring opposite sides of the fuel assembly simultaneously. Each arm contains an ionization chamber operating in the current mode to measure the total gamma-ray output and two fission chambers operating in the pulse mode to measure the total neutron output. In each arm, one fission chamber is wrapped in cadmium and one is bare. If it is necessary to determine the boron content of the water (typically 2000 ppm) to correct the neutron count rate, this can be done with the ratio of counts in the bare and cadmium-wrapped fission chambers (Refs. 31 and 32). The fork detector is available with two different apertures, one for PWR and one for BWR assemblies.

The ION-1 electronics package is a battery-powered, microprocessor-based unit that performs internal diagnostics and assists the inspector with data collection and analysis (Ref. 33). If measurements are to be made along the vertical length of the fuel assembly in order to obtain an axial burnup profile, the ION-1 can step the inspector through the scanning procedure.

---



**Fig. 18.18** Schematic of an irradiated-fuel measurement system for total neutron and total gamma-ray measurements. The system consists of an ION-1 electronics package, a long cable boom, and a fork detector.

Most measurements with the ION-1 electronics package and fork detector are made only at the axial midpoint of the fuel assembly. An average of 5 to 7 min is required to (1) position the fuel-handling bridge, (2) raise the fuel assembly partially out of the storage rack, (3) perform the measurements, and (4) replace the fuel assembly in the storage rack. Including time for assembly and disassembly of equipment, a measurement campaign at a reactor storage pond typically requires 2 to 3 days. With proper calibration, the fork detector can determine the burnup of individual fuel assemblies to about 5%.

### 18.5.2 Neutron Measurement of Burnup

Measurement results from a BWR irradiated-fuel storage facility are shown in Figure 18.20. The measured neutron activity of 36 BWR fuel assemblies is plotted as a function of declared exposure, which varied from 8.5 to 29 GWd/tU. One fuel assembly with a noncontinuous irradiation is clearly identified as an outlier. This particular fuel assembly had been irradiated to 18.0 GWd/tU, placed in the storage pond for 3 yr, and then returned to the reactor for an additional 3 GWd/tU exposure. During the 3-yr interim between exposures, the  $^{241}\text{Pu}$  decayed to form  $^{241}\text{Am}$ , which in turn yielded large quantities of  $^{242}\text{Cm}$  when the fuel was returned to the reactor (see Section 18.3.6).



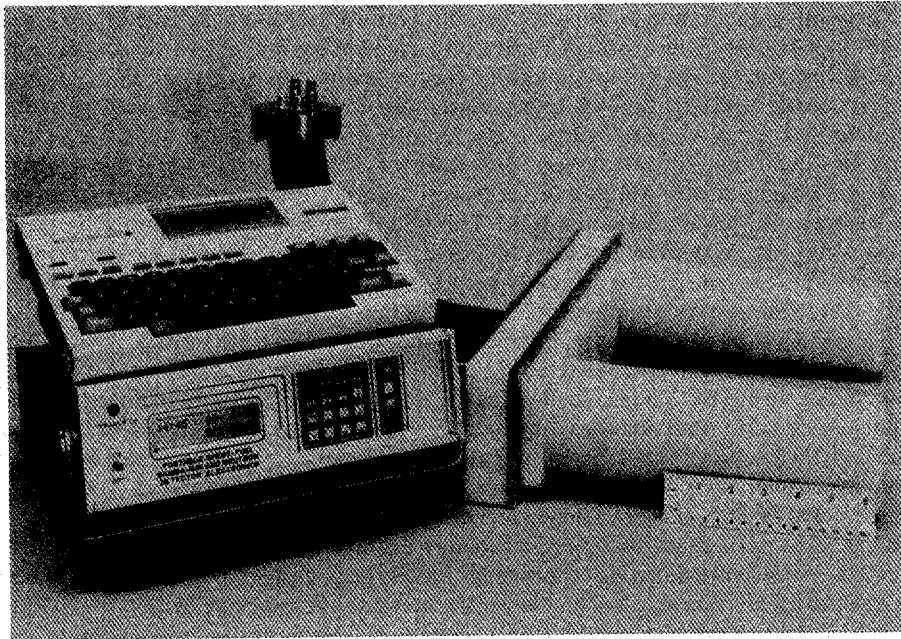


**Fig. 18.19** The ION-1 electronics package and the fork detector.

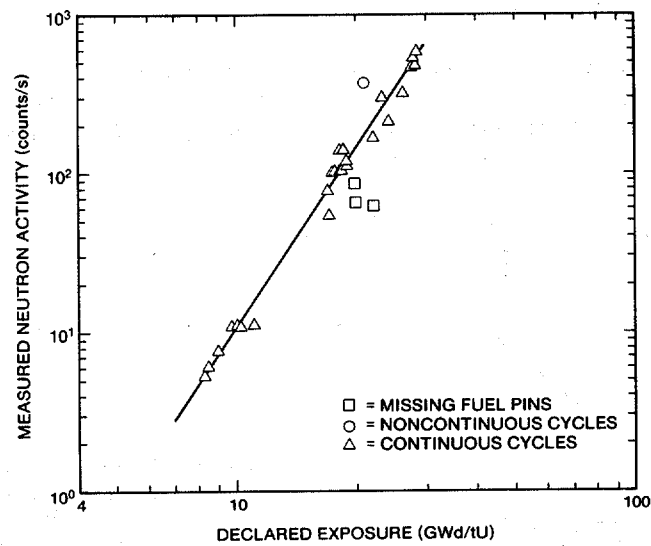


**Fig. 18.20** Measured neutron activity of 36 irradiated BWR fuel assemblies plotted as a function of declared exposure. The solid line is a power function fit to the experimental data.

Three other data points in Figure 18.20 lie significantly below the fitted line. These assemblies had been reconstituted from other assemblies having various exposures. Also, several fuel pins were missing from each of these fuel assemblies. Both of these factors contributed to the lower measured neutron emission rates. If the reconstituted assemblies and the assembly with the noncontinuous irradiation history are excluded from the data analysis, an average difference of 3.0% exists between the declared exposure values and the values obtained from a power function relationship between count rate and exposure (Equation 18-4). This power function was determined by a least squares fit of the experimental data, and yields  $\beta = 3.7$ . By applying a correction for cooling time, the data for the assembly with the noncontinuous irradiation history can also be brought into good agreement.

Figure 18.21 shows neutron measurements made at a PWR fuel storage facility. The response of 17 irradiated fuel assemblies is plotted as a function of declared exposure, which varied from 25 to 35 GWd/tU. These data identify an enrichment effect that was predicted by burnup calculations, as described in Section 18.3.6. Four assemblies with initial  $^{235}\text{U}$  enrichments of 2.4% have significantly higher neutron count rates compared with assemblies with identical exposures and cooling times but with initial  $^{235}\text{U}$  enrichments of 3.6%. Lower-enriched fuel has less fissile material and therefore requires a higher neutron fluence to achieve the same exposure level as higher-enriched fuel. From the figure it is evident that the data for fuel with an initial enrichment of 3.6% form an excellent power law relationship between count rate and exposure, with  $\beta = 3.9$ . The operator-declared exposures differ from calculated values by an average of 0.9%.

## 18.6 DETERMINATION OF THE FISSILE CONTENT OF IRRADIATED FUEL

Sections 18.4 and 18.5 have described a variety of passive nondestructive measurement techniques for irradiated fuel materials. Each of these techniques provides an indirect measure of fuel burnup. Neither the unique gamma-ray signatures nor the

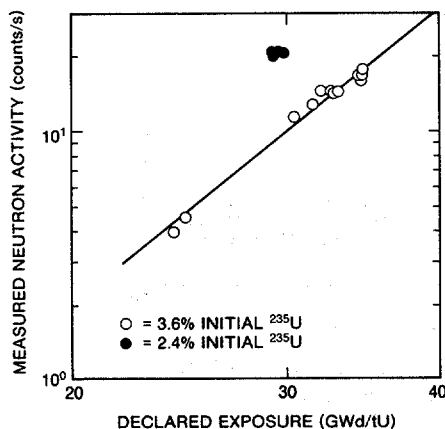


**Fig. 18.21** Measured neutron activity of 17 irradiated PWR fuel assemblies plotted as a function of declared exposure. The solid line is a power function fit to the assemblies having an initial enrichment of 3.6%.

neutron signatures of the uranium or plutonium isotopes can be measured directly. To determine the actual concentration of fissile material, there are two possible approaches. One method uses calculated or empirically determined correlations to relate burnup to residual  $^{235}\text{U}$  and plutonium content. The other method uses active neutron interrogation to override the passive neutron signal and obtain a net induced response from the fissile isotopes. Both methods are currently being developed by investigators in several countries. The methods are described briefly in the remainder of this section.

### 18.6.1 Indirect Determination from Passive Burnup Measurements

Most passive nondestructive measurements of irradiated fuel in the field are now limited to verification of the relative burnup levels of the assemblies. Within the constraints of time and manpower, it is customary to measure as many assemblies as possible, but most assemblies are measured at only one position along their length. If the measurements at this position are representative, the relative burnups of the assemblies can be obtained. Previously established correlations between burnup and the passive radiation levels then verify that the measurements are consistent with operator-declared values for burnup and cooling time. (Operator-declared values for burnup are only good to about 5% because of variations in core parameters.) Because it is very difficult to remove fissile material from the assemblies without also removing the fission product radiation sources, this verification implies that the fissile material is intact.

In principle, the fissile content of the fuel can be determined indirectly from the measured gamma-ray and neutron signals. First, it would be necessary to obtain an absolute value for the fuel burnup by destructive analysis of a section of the fuel. Then high-resolution gamma-ray measurements of single fission product activities or fission product activity ratios could be normalized to the destructive analysis to obtain an absolute calibration. Neutron measurements could also be related to the absolute burnup. Both neutron and gamma-ray measurements would have to be integrated along the axial profiles of the fuel assemblies to correct for variations in burnup. If an absolute calibration performed at one facility were used at another facility, the calibration would have to be adjusted for a variety of reactor-specific parameters including fuel enrichment, power history, and moderator and poison concentrations. Some examples of the influence of such parameters are given in Sections 18.3.5 and 18.3.6.

If absolute values for fuel burnup can be established, the concentration of fissile isotopes can be obtained by calculation. These calculations are usually carried out by complex computer codes such as CINDER (Refs. 6 and 7). An example of the result of such a calculation is given in Figure 18.22, which plots the concentration of the plutonium isotopes as a function of burnup. The accuracy of such computer codes for uranium and plutonium is typically 5 to 10%. If the reactor operating history is not known, the error may increase by an additional 5 to 15% (Ref. 11).

This indirect determination of fissile content from passive radiation measurements is very difficult because of the many measurement variables and reactor core parameters involved. Indirect correlation of fissile content with passive measurements is vulnerable to uncertainty, whereas direct correlation of fuel integrity with measurement is now a well-established and reliable technique.

---

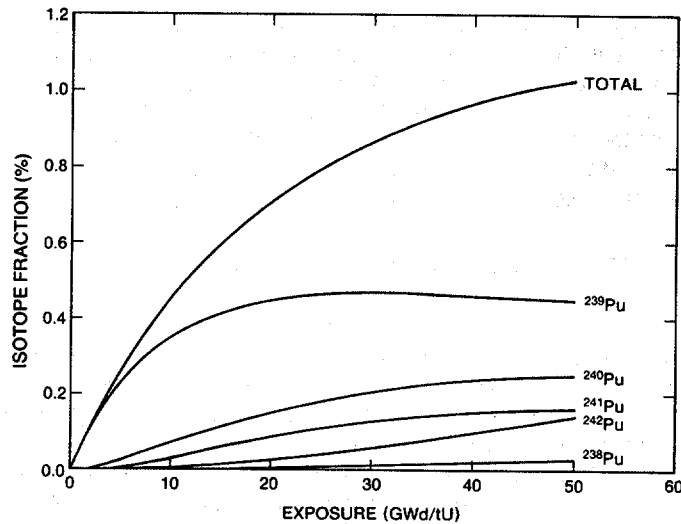


Fig. 18.22 Relative concentrations of the plutonium isotopes (expressed as weight percent of initial uranium) as a function of exposure. The data were obtained by calculation with the EPRI-CINDER Code (Ref. 5).

### 18.6.2 Determination by Active Neutron Interrogation

A direct measurement of the fissile content of irradiated fuel is possible using a large neutron source to induce fissions. The source can be an accelerator, a 14-MeV neutron generator, or an isotopic source like RaBe, SbBe, or californium. The source is positioned near the irradiated fuel, where it produces an induced fission signal proportional to the amount of fissile material. Typical neutron source strengths must be on the order of  $10^8$  to  $10^9$  n/s to induce a fission signal that is comparable in size to the passive neutron yield. In practice, active neutron interrogation systems cannot distinguish between uranium and plutonium. The induced fission response is proportional to the total fissile mass of  $^{235}\text{U}$ ,  $^{239}\text{Pu}$ , and  $^{241}\text{Pu}$ .

A combined active and passive neutron assay system has been developed by G. Schulze, H. Wuerz, and others (Ref. 19) using a  $^{252}\text{Cf}$  source. The system can determine fuel burnup and initial uranium content. The plutonium content can be obtained indirectly from isotopic correlations.

Several facilities have used the delayed neutron activation technique to measure irradiated fuel. The reprocessing facility at Dounreay, United Kingdom, has used a 14-MeV neutron generator to assay baskets of leached hulls (Ref. 34). Recently this assay system was converted to a californium Shuffler for the neutron interrogation (Ref. 35). A large californium Shuffler system has also been developed for the assay of highly enriched irradiated uranium (Ref. 36). However, at the present time there are no active neutron systems in operation to measure power reactor fuel assemblies. This is because

active neutron systems require an accelerator or neutron generator or a large, heavily shielded isotopic source, which has limited the use of these systems to fixed, in-plant installations in research laboratories or reprocessing facilities. The status of active neutron techniques and measurement results is summarized in Refs. 4 and 11.

## 18.7 SUMMARY OF NONDESTRUCTIVE TECHNIQUES FOR VERIFICATION OF IRRADIATED FUEL

Table 18-6 summarizes the nondestructive assay techniques available for the verification of irradiated-fuel assemblies. Depending on the level of verification needed, an inspector might use one or more of the gamma-ray or neutron techniques described in this chapter. In general, the most effective verification would be obtained by a combination of gamma-ray and neutron techniques.

### REFERENCES

1. *Nucleonics Week*, January 2, 1986.
  2. Duderstadt and Hamilton, *Nuclear Reactor Analysis* (John Wiley and Sons, Inc., New York, 1976).
  3. A. V. Nero, *A Guidebook to Nuclear Reactors* (University of California Press, Berkeley, California, 1979).
  4. T. D. Reilly, "The Measurement of Leached Hulls," Los Alamos Scientific Laboratory report LA-7784-MS (1979).
  5. G. E. Bosler, J. R. Phillips, W. B. Wilson, R. J. LaBauve, and T. R. England, "Production of Actinide Isotopes in Simulated PWR Fuel and Their Influence on Inherent Neutron Emission," Los Alamos National Laboratory report LA-9343 (1982).
  6. T. R. England, W. B. Wilson, and M. G. Stamatelatos, "Fission Product Data for Thermal Reactors, Part 1: A Data Set for EPRI-CINDER Using ENDF/B-IV," Electric Power Research Institute report EPRI NP/356, Part 1, and Los Alamos Scientific Laboratory report LA-6745-MS (1976).
  7. T. R. England, W. B. Wilson, and M. G. Stamatelatos, "Fission Product Data for Thermal Reactors, Part 2: Users Manual for EPRI-CINDER Code and Data," Electric Power Research Institute report EPRI NP/356, Part 2, and Los Alamos Scientific Laboratory report LA-6746-MS (1976).
-

Table 18-6. Nondestructive assay techniques for verification of irradiated-fuel assemblies

Special Level of Verification	Measurement Technique		
	Gamma Ray	Neutron	Instrumentation
Physical characteristics			Visual inspection
Indication of irradiation exposure	Cerenkov		Cerenkov viewing device
	Presence of gamma radiation		Ion chambers Thermoluminescence detectors Scintillators
Physical integrity of fuel assembly		Presence of neutron radiation	Fission chambers <sup>10</sup> B detectors
	Cerenkov		Cerenkov viewing device
	Relative intensities of high-energy gamma rays		Germanium detector Be( $\gamma$ ,n) detector
Presence of fission products and actinides		Relative values of neutron emission rates	Fission chambers <sup>10</sup> B detectors
	Qualitative identification of specific gamma-ray lines		Germanium detector Be( $\gamma$ ,n) detector
		Relative values of neutron emission rates	Fission chambers <sup>10</sup> B detectors

Table 18-6. (cont.)

Special Level of Verification	Measurement Technique		Instrumentation
	Gamma Ray	Neutron	
Relative concentrations of fission products and actinides	Quantitative measure- ment of $^{137}\text{Cs}$ , $^{134}\text{Cs}$ / $^{137}\text{Cs}$ , and $^{154}\text{Eu}/^{137}\text{Cs}$ ; correlation with operator- declared information		Germanium detectors
			Quantitative measure- ment of neutron emis- sion rate; correlation with operator-declared information
Direct measurement of fissile content	Indirectly through cor- relations between NDA measurements and de- structive analyses		Germanium detectors
			Quantitative measure- ment of induced fis- sions in special nuclear material

8. D. Cobb, J. Phillips, G. Bosler, G. Eccleston, J. Halbig, C. Hatcher, and S. T. Hsue, "Nondestructive Verification and Assay Systems for Spent Fuels," Los Alamos National Laboratory report LA-9041, Vol. 1 (April 1982).
  9. E. J. Dowdy, N. Nicholson, and J. T. Caldwell, "Irradiated Fuel Monitoring by Cerenkov Glow Intensity Measurements," Los Alamos Scientific Laboratory report LA-7838-MS (1979).
  10. N. Nicholson and E. J. Dowdy, "Irradiated Fuel Examination Using the Cerenkov Technique," Los Alamos National Laboratory report LA-8767-MS (1981).
  11. S. T. Hsue, T. W. Crane, W. L. Talbert, and J. C. Lee, "Nondestructive Assay Methods for Irradiated Nuclear Fuels," Los Alamos Scientific Laboratory report LA-6923 (1978).
  12. J. R. Phillips, G. E. Bosler, J. K. Halbig, S. F. Klosterbuer, and H. O. Menlove, "Nondestructive Verification with Minimal Movement of Irradiated Light-Water Reactor Fuel Assemblies," Los Alamos National Laboratory report LA-9438-MS (1982).
  13. P. M. Rinard, "A Spent-Fuel Cooling Curve for Safeguard Applications of Gross-Gamma Measurements," Los Alamos National Laboratory report LA-9757-MS (1983).
  14. Advisory Group Meeting on the Nondestructive Analysis of Irradiated Power Reactor Fuel, International Atomic Energy Agency report AG-241 (October 29-November 2, 1979).
  15. J. R. Phillips, B. K. Barnes, and T. R. Bement, "Correlation of the Cesium-134/Cesium-137 Ratio to Fast Reactor Burnup," *Nuclear Technology* 46, 21 (1979).
  16. J. R. Phillips, J. K. Halbig, D. M. Lee, S. E. Beach, T. R. Bement, E. Dermendjiev, C. R. Hatcher, K. Kaieda, and E. G. Medina, "Application of Nondestructive Gamma-Ray and Neutron Techniques for the Safeguarding of Irradiated Fuel Materials," Los Alamos Scientific Laboratory report LA-8212 (1980).
  17. S. T. Hsue, C. R. Hatcher, and K. Kaieda, "Cooling Time Determination of Spent Fuel," *Nuclear Materials Management* 8, 356-367 (Fall 1979).
  18. A. J. G. Ramalho and W. E. Payne, "Spent Fuel Measurements Using High-Resolution Gamma Systems," *Nuclear Materials Management* 8, 76 (1979).
-



19. G. Schulze, H. Wuerz, L. Koch, and R. Wellum, "Neutron Assay Plus Isotopic Correlations: A Method for Determining Pu and Burnup in Spent LWR Fuel Assemblies," *Proc. Second Annual Symposium on Safeguards and Nuclear Materials Management*, Edinburgh, Scotland, March 26-28, 1980 (European Safeguards Research and Development Association, Brussels, Belgium, 1980), pp. 396-403.
  20. J. R. Phillips, G. E. Bosler, J. K. Halbig, S. F. Klosterbuer, D. M. Lee, and H. O. Menlove, "Neutron Measurement Techniques for the Nondestructive Analysis of Irradiated Fuel Assemblies," Los Alamos National Laboratory report LA-9002-MS (1981).
  21. P. Fedotov, N. M. Kazarinov, and A. A. Voronkov, "The Use of Neutron Scanning Method for Analysis of Spent VVER Assemblies in Safeguarding Systems," presented at the IAEA Advisory Group Meeting on Methods and Techniques for NDA Safeguards Measurements of Power Reactor Spent Fuel, Vienna, October 28-November 2, 1979.
  22. S. T. Hsue, J. Stewart, K. Kaieda, J. Halbig, J. Phillips, D. Lee, and C. Hatcher, "Passive Neutron Assay of Irradiated Nuclear Fuels," Los Alamos Scientific Laboratory report LA-7645-MS (1979).
  23. J. R. Phillips and G. E. Bosler, "Calculated Response Contribution of Gamma Rays Emitted from Fuel Pins in an Irradiated PWR Fuel Assembly," Los Alamos National Laboratory report LA-9837 (1983).
  24. R. J. S. Harry, J. K. Aaldijk, and J. P. Braak, "Gamma Spectrometric Determination of Isotopic Composition Without Use of Standards," in *Proceedings of the International Symposium on Nuclear Materials Safeguards*, Vienna, October 20-24, 1975 (IAEA-SM-201/68).
  25. T. N. Dragnev, "Intrinsic Self-Calibration of Nondestructive Gamma Spectrometric Measurements (Determination of U, Pu, and Am-241 Isotopic Ratios)," International Atomic Energy Agency report IAEA/STR-60 (1976).
  26. T. R. Bement and J. R. Phillips, "Evaluation of Relative Detection Efficiency on Sets of Irradiated Fuel Elements," *Proc. of the 1980 DOE Statistical Symposium*, October 29-31, 1980 (CONF-801045).
  27. T. Suzaki, H. Tsuruto, and S. Matura, "Non-Destructive Gamma-Ray Spectrometry and Analysis on Spent Fuel Assemblies of the JPDR-I Core," Japan Atomic Energy Research Institute report JAERI-memo 8164 (1979).
-

28. C. E. Moss and D. M. Lee, "Gross Gamma-Ray Measurements of Light-Water Reactor Spent-Fuel Assemblies in Underwater Storage Arrays," Los Alamos Scientific Laboratory report LA-8447 (1980).
  29. J. R. Phillips, G. E. Bosler, J. K. Halbig, S. F. Klosterbuer, H. O. Menlove, and P. M. Rinard, "Experience Using a Spent-Fuel Measurement System," presented at the 24th Annual Meeting of the Institute of Nuclear Materials Management, Vail, Colorado, July 10-13, 1983.
  30. R. N. Olsen, Ed., "Instructions for the Use of the ION-1 and the Fork Detector," International Atomic Energy Agency report IMI No. 42 (November 1984).
  31. P. M. Rinard, "Neutron Measurements in Borated Water for PWR Fuel Inspections," Los Alamos National Laboratory report LA-10068-MS (1984).
  32. P. M. Rinard and G. E. Bosler, "BWR Spent-Fuel Measurements with the ION-1/Fork Detector and Calorimeter," Los Alamos National Laboratory report LA-10758-MS (1986).
  33. S. Klosterbuer and J. Halbig, "Portable Spent-Fuel Gamma-Ray and Neutron Detector Electronics User Manual," Los Alamos National Laboratory report LA-8707-M (1983).
  34. B. McDonald, G. Fox, and W. Bremner, "Nondestructive Measurements of Plutonium and Uranium in Process Wastes and Residues," in *Safeguarding Nuclear Materials*, Proc. Symp., Vienna, 1975 (IAEA Pub 408, Vol. II, p. 589, 1976).
  35. G. Eccleston, H. Menlove, T. Van Lyssel, G. Walton, D. C. Garcia, and G. Ortiz, "Dounreay Shuffler," in "Safeguards and Security Progress Report, January-December 1983," Los Alamos National Laboratory report LA-10170 (September 1984), p. 59.
  36. G. W. Eccleston, H. O. Menlove, and M. W. Echo, "A Measurement Technique for High Enrichment Spent Fuel Assemblies and Waste Solids," *Nuclear Materials Management* 8, 344-355 (1979).
-